Dynamical and Rheological Properties of Fluorinated Surfactant Films Adsorbed at the Pressurized CO2−H2O Interface

ARTICLE *in* LANGMUIR · JUNE 2011

Impact Factor: 4.46 · DOI: 10.1021/la201009z · Source: PubMed

3 AUTHORS:

Frederic Tewes
Université de Poitiers
31 PUBLICATIONS **363** CITATIONS
SEE PROFILE

Marie Pierre Krafft
University of Strasbourg
169 PUBLICATIONS **3,487** CITATIONS
SEE PROFILE

Frank Boury
University of Angers
100 PUBLICATIONS **1,744** CITATIONS
SEE PROFILE

Langmuir

ARTICLE

pubs.acs.org/Langmuir

Dynamical and Rheological Properties of Fluorinated Surfactant Films Adsorbed at the Pressurized CO_2−H_2O Interface

Frederic Tewes,[§,∥] Marie Pierre Krafft,[‡] and Frank Boury*[,†]

[†]Lunam Université, université d'Angers, Ingénierie de la Vectorisation Particulaire, INSERM U 646, IBS Institut de Biologie en Santé, 4 rue Larrey, 49933 Angers, France

[‡]Systèmes Fluorés Organisés à Finalités Thérapeutiques (SOFFT), Université de Strasbourg, Institut Charles Sadron, UPR CNRS 22, 23 rue du Loess, 67034 Strasbourg Cedex, France

[§]School of Pharmacy and Pharmaceutical Sciences, University of Dublin, Trinity College, Dublin 2, Ireland

[∥] Faculté de Médecine & Pharmacie, INSERM ERI-23, Pôle Biologie-Santé, Université de Poitiers, 40 av. du Recteur Pineau, 86022 Poitiers Cedex, France

ABSTRACT:

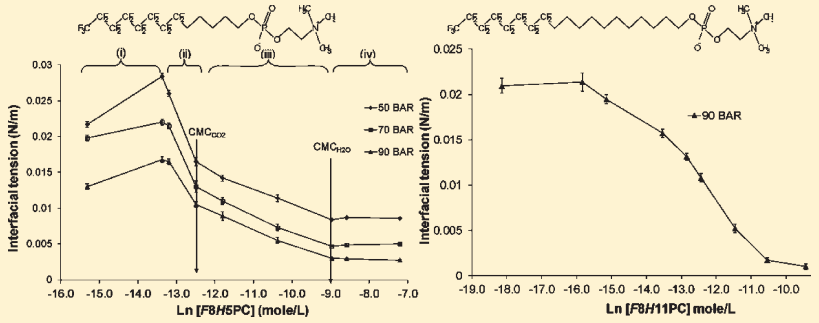

The dynamics of adsorption, interfacial tension, and rheological properties of two phosphocholine-derived partially fluorinated surfactants *FnHm*PC, designed to compensate for the weak CO_2−surfactant tail interactions, were determined at the pressurized CO_2−H_2O interface. The two surfactants differ only by the length of the hydrocarbon spacer (5 CH_2 in *F8H5*PC and 11 CH_2 in *F8H11*PC) located between the terminal perfluoroalkyl chain and the polar head. The length of this spacer was found to have a critical impact on the adsorption kinetics and elasticity of the interfacial surfactant film. *F8H5*PC is soluble in both water and CO_2 phases and presents several distinct successive interfacial behaviors when bulk water concentration (C_W) increases and displays a nonclassical isotherm shape. The isotherms of *F8H5*PC are similar for the three CO_2 pressures investigated and comprise four regimes. In the first regime, at low C_W, the interfacial tension is controlled by the organization that occurs between H_2O and CO_2. The second regime corresponds to the adsorption of the surfactant as a monolayer until the CO_2 phase is saturated with *F8H5*PC, resulting in a first inflection point. In this regime, *F8H5*PC molecules reach maximal compaction and display the highest apparent interfacial elasticity. In the third regime, a second inflection is observed that corresponds to the critical micelle concentration of the surfactant in water. At the highest concentrations (fourth regime), the interfacial films are purely viscous and highly flexible, suggesting the capacity for this surfactant to produce water-in-CO_2 microemulsion. In this regime, surfactant adsorption is very fast and equilibrium is reached in less than 100 s. The behavior of *F8H11*PC is drastically different: it forms micelles only in the water phase, resulting in a classical Gibbs interface. This surfactant decreases the interfacial tension down to 1 mN/m and forms a strongly elastic interface. As this surfactant forms a very cohesive interface, it should be suitable for formulating stable water-in-CO_2 emulsions. The finding that the length of the hydrocarbon spacer in partially fluorinated surfactants can drastically influence film properties at the CO_2−H_2O interface should help control the formation of microemulsions versus emulsions and help elaborate a rationale for the design of surfactants specifically adapted to pressurized CO_2.

1. INTRODUCTION

The vast potential of CO_2 as an environmentally safe and tunable solvent is being actively investigated in numerous applications. For example, pressurized CO_2 was used as a reaction medium,[1] as the continuous phase of emulsions[2−4] and microemulsions,[5] or for the synthesis of particles.[6] Its low critical parameters (T_c = 31.1 °C and P_c = 73.8 bar) make CO_2 a valuable alternative for toxic and environmentally harmful organic solvents.

However, despite their advantages, the development of CO_2-based processes is hindered by the fact that CO_2 is a poor solvent for hydrophilic substances. CO_2 is a symmetrical molecule, with a statistically null dipole moment, which results in very weak interactions with polar compounds. Furthermore, the polarizability of

Received: March 17, 2011
Revised: May 15, 2011
Published: June 01, 2011

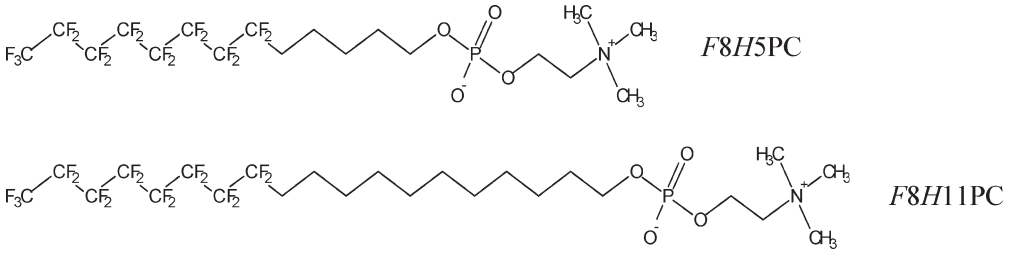

Figure 1. *F8H5*PC and *F8H*11PC surfactant structures.

CO_2 is low, resulting in weak dispersion forces (e.g., van der Waals interactions) and weak interaction with apolar substances. Thus, CO_2 can only solubilize low molecular weight apolar compounds. In order to overcome this major limitation, water-in-CO_2 (W/C) emulsions or microemulsions have been formulated.[3,5,7,8] Because of their binary composition, these systems provide new approaches for processing biological compounds[9−11] and formulate micro- and nanoparticles.[6]

According to Bancroft's rule, dispersion of H_2O in a CO_2 continuous phase requires surfactants that have a CO_2-philic tail and a packing parameter that can minimize the curvature energy. Additionally, the water droplets are in constant motion in these dispersions, and in the absence of a sterical and/or electrical barrier, they collide frequently, which can lead to droplet aggregation and, eventually, to their irreversible coalescence. As CO_2 has a low dielectric constant, it is difficult to create an electrostatic barrier. A sterical barrier can be formed by a film of surfactant molecules adsorbed at the interface that extend their tails into the continuous phase. However, in W/C emulsions, it is very difficult to produce this kind of barrier because few surfactants are soluble enough in CO_2. One notable exception consists of fluorinated surfactants (*F*-surfactants)[4,12−14] and, to a lesser extent, siloxanes[15] and polycarbonate surfactants.[16] In fact, CO_2 interacts preferentially with substances having low polarizability, in particular with fluorocarbons and perfluoroalkyl chains. These interactions are rather weak and involved F−CO_2 site-specific Lewis base−Lewis acid interaction.[17] Several studies report dispersions of water droplets in a CO_2 phase using *F*-surfactants, including hybrid surfactants with one fluorocarbon and one hydrocarbon chain,[18,19] including fluoroethers,[2] fluorinated aerosol-OT (AOT, sodium bis(2-ethylhexyl)sulfosuccinate) analogues, or fluorinated phosphates. Harrison et al.[18] were among the first to describe the formation of a W/C microemulsion, at 35 °C and for a CO_2 pressure (P_{CO_2}) of 260 bar, using the hybrid surfactant $(C_7F_{15})(C_7H_{15})CHSO_4^-$,$Na^+$. Eastoe et al.[5,20] obtained a W/C microemulsion at 15 °C and 566 bar using the partially fluorinated AOT analogue bis(1*H*,1*H*,5*H*-octafluoropentyl)-2-sulfosuccinate. Perfluoropolyether (PFPE) carboxylates have also been extensively used to stabilize W/C microemulsions.[7,21] da Rocha et al.[22] were the first to report on the thermodynamics of microemulsion formation with a perfluoroalkylated surfactant in a compressible fluid, demonstrating that microemulsion formation was enthalpy driven. In another study, da Rocha et al.[3] compared the decrease in interfacial tension (γ) obtained with PFPE-$COONH_4^+$, fluoroether sulfate, fluoroether sorbitol, and block copolymers. They concluded that PFPE-$COONH_4^+$ can lower γ down to a value of 0.8 mN/m, which makes possible the formation of a microemulsion.

Strikingly, the literature provides few data about the elasticity of surfactant films at the CO_2−H_2O interface. Yet, such knowledge is useful for predicting the capacity of a surfactant to stabilize W/C emulsions or microemulsions. It is one of the purposes of this work to provide such fundamental information and to explore whether manipulation of surfactant structure can impact film elasticity at the CO_2−H_2O interface.

A large variety of well-defined fluorosurfactants have been synthesized and investigated by Krafft et al.[23−25] Stepwise structural changes in head groups, fluorocarbon chains, and spacer length allow gradual modification of surfactant properties. The formation and properties of water-in-fluorocarbon emulsions and microemulsions destined for pulmonary drug administration were strongly related to the length of the hydrocarbon spacer within the surfactant.[26] It has also been shown that the effect of such a spacer does not follow a simple rule.[27]

In this paper we present the adsorption kinetics and interfacial rheological properties of two partially fluorinated surfactants (Figure 1) derived from phosphocholine adsorbed at the H_2O−pressurized CO_2 interface. These surfactants differ only by the length of their hydrocarbon spacer, i.e., 5 CH_2 groups for *F8H5*PC and 11 CH_2 groups for *F8H*11PC, allowing assessment of the effect of spacer length on surfactant film characteristics at this interface.

The influence of a hydrocarbon spacer on film thermodynamics has never been explored. While γ measurements have been published for some *F*-surfactants at the CO_2−H_2O interface,[3,22] no study of the interfacial rheology of *F*-surfactant films has yet been reported at this interface. Our measurements allow evaluation of the ability for these surfactants to form and stabilize H_2O-in-CO_2 emulsions or microemulsions.

2. MATERIALS AND METHODS

2.1. Materials. The measuring cell was filled with CO_2 (purity 99%) (Air liquide, France). Ultrapure water was produced by a Milli-Q plus 188 apparatus (Millipore, France). The phosphocholine-based partially *F*-surfactants were synthesized according to Krafft et al.[28] Their purity (>99%) was assessed by HPLC, NMR, and elemental analysis.

2.2. Pendant Drop Tensiometer. The drop tensiometer (Tracker, Teclis, Longessaigne, France) determines γ by analyzing the axial symmetric shape (Laplacian profile) of the pendant drop (aqueous phase) in CO_2. The apparatus consists of a view cell placed in a CO_2 atmosphere, a light source, a CCD camera, a computer, a syringe, and a motor as described by Tewes et al.[29−31] The syringe was filled with aqueous solutions of *F8H5*PC or *F8H*11PC with surfactant bulk concentrations (C_W) ranging from 1×10^{-4} to 1×10^{-10} M and coupled to the view cell. Then, the view cell was pressurized with pure CO_2 until reaching the desired temperature (40 °C) and pressure, after which the water and CO_2 phases were allowed to equilibrate for 12 h. Pendant drops, whose area was controlled during the whole observation time by a step-by step motor, were formed at the extremity of a stainless steel tube (internal diameter 1 mm) connected to a syringe. The

dx.doi.org/10.1021/la201009z |*Langmuir* 2011, 27, 8144–8152

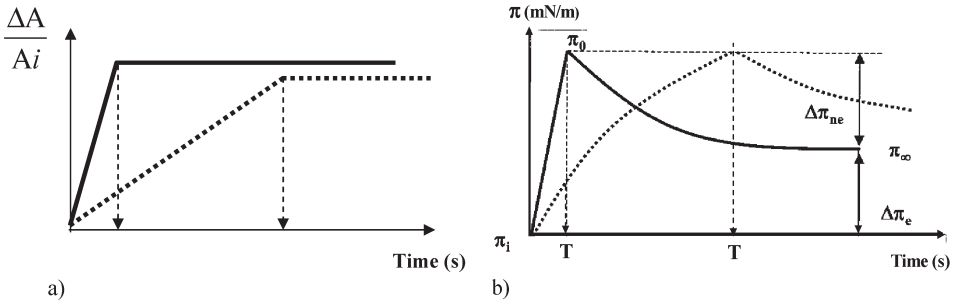

Figure 2. (a) Relative area compression and (b) surface pressure variation $\Delta\pi$ over time T for fast (bold line) and slow (dashed line) compressions.

interfacial tension was determined by analyzing the profile of the droplet using a CCD camera, coupled to a video image profile digitizer board connected to a computer.

2.3. Interfacial Rheology Measurements. The principle of the rheological experiments is to apply a controlled perturbation to the droplet surface and monitor the resulting surface pressure (π) variations. The dynamic response of the interfacial film to a dilatational mechanical strain on the time scale of $1-10^3$ s was studied by means of a ramp-type perturbation approach. This approach consists in realizing two types of continuous and monotonic compressions of the equilibrated surface layer of the pendant drop: a slow compression (Figure 2a, dashed line) and a fast compression (bold line). Simultaneously, the variation of the interfacial pressure during the slow compression (dashed line) or after the fast compression was measured in order to determine the relaxation of the interface (bold line).

A convenient theoretical model (generalized Maxwell model), corresponding to a solid viscoelastic body, has been applied to various interfacial systems (phospholipids or polymers).[30,32,33]

In order to describe the surface pressure variation $\Delta\pi = \pi(t) - \pi i$ (i.e., the resulting stress; Figure 2b) during the time T of the compression at a constant velocity U_b, it is supposed that at any moment

$$\Delta\pi = \Delta\pi_e + \Delta\pi_{ne} \quad (1)$$

where $\Delta\pi_e$ and $\Delta\pi_{ne}$ are the equilibrium and nonequilibrium contributions to the stress. $\Delta\pi_e$ depends on the equilibrium surface dilatational elasticity (E_e) according to eq 2:

$$\Delta\pi_e = E_e\frac{U_b t}{A_i} \quad (2)$$

where A_i is the initial surface area before the mechanical strain ($U_b t/A_i \equiv \Delta A/A_i$). The nonequilibrium part of the resulting stress, $\Delta\pi_{ne}$, is correlated to the accumulation of elastic energy during compression. Dissipation of the accumulated energy occurs during compression as well as during relaxation and can be interpreted as a molecular reorganization in the interface. This viscoelastic behavior can be described using eq 3:

$$\frac{d\Delta\pi_{ne}}{dt} + \frac{\Delta\pi_{ne}}{\tau} = E_{ne}\frac{U_b}{A_i} \quad (3)$$

where E_{ne} is the nonequilibrium surface dilatational elasticity and τ the specific relaxation time. If the initial conditions are $\Delta\pi_{ne} = 0$ at $t = 0$, $\Delta\pi_{ne}$ can be written

$$\Delta\pi_{ne} = \frac{E_{ne}U_b t}{A_i}(1 - e^{-t/\tau}) \quad (4)$$

As the stresses are additives, the viscoelastic behavior of the interfacial monolayer is described by eq 5:

$$\frac{\Delta\pi}{U_b t}A_i = E_e + E_{ne}\frac{\tau}{t}(1 - e^{-t/\tau}) \quad (5)$$

τ was determined from fast compressions ($d/dt\ \Delta A(t)/A_i = U_b/A_i$ typically higher than 0.005 s^{-1}, with $\Delta\pi_{max} < 2$ mN/m) where the compression time T is much smaller than the characteristic time of the relaxation process τ. Subsequently, this characteristic relaxation time is determined by fitting the γ relaxation curves by an exponential equation: $\gamma = \gamma_\infty + Ae^{-t/\tau}$. Slow compressions ($d/dt\ \Delta A(t)/A_i = U_b/A_i$ typically lower than 0.003 s^{-1}, with $\Delta\pi_{max} < 2$ mN/m) were performed in order to determine the compression relaxation part. The value of τ and eq 5 are used to determine E_e and E_{ne}.

3. RESULTS AND DISCUSSION

3.1. Interfacial Tension Measurements. Figure 3 shows γ variation kinetics obtained at a P_{CO2} of 90 bar in the presence of *F8H5*PC (A) and *F8H11*PC (B) for various surfactant concentrations in bulk water (C_W). For *F8H5*PC, kinetics acquired with C_W values larger than 1.3×10^{-4} M reached the equilibrium state very quickly (<50 s). Those acquired with C_W lower than 1.3×10^{-4} M required 20 000 s or more to reach equilibrium. This sharp difference in γ kinetics profiles suggests that the surfactant molecules are brought in different ways to the interface, depending on concentration. For *F8H11*PC, the time needed to reach equilibrium interfacial tension (γ_{eq}) decreased gradually with the increase in C_W. No abrupt change was observed.

The γ_{eq} values measured at the CO_2-H_2O interface for different *F*-surfactant C_W values were used to plot Gibbs isotherms (γ_{eq} vs ln C_W, Figure 4). By comparing the isotherms obtained with the two surfactants at a P_{CO2} of 90 bar, it appears that *F8H11*PC is able to reduce γ_{eq} to a lower minimal value (1 mN/m) than *F8H5*PC. Hence, similarly to the adsorption of semifluorinated alkanes at the alkane/air interface,[23] increasing the chain length resulted in increased γ reduction effectiveness.

The shape of the isotherms obtained with *F8H5*PC at different P_{CO_2} was not conventional and revealed different interfacial behaviors, depending on *F8H5*PC C_W. The various regimes observed are numbered from (i) to (iv) in Figure 4A.

(i) The first regime is observed for $C_W < 1 \times 10^{-6}$ M. For these C_W values, γ_{eq} values are abnormally low, as an increase in C_W lead to an increase in γ_{eq}. This could be related to the organization that occurs between water and pressurized CO_2.[34] The interfacial tension between pure H_2O and pure CO_2 was indeed shown to decrease over time due to the formation of a structured interface with pressure-dependent properties.[29] At very low *F8H5*PC C_W, the effect of this organization on γ should be predominant and could hide or inhibit the effect of surfactant adsorption. Above a given concentration, fast adsorption of the *F*-surfactant could disturb or hinder the CO_2-H_2O organization, as observed for ovalbumin adsorption at the CO_2-H_2O interface.[30]

(ii) A second regime was observed for *F8H5*PC C_W values comprised between 1.6×10^{-6} and 4×10^{-6} M, in which γ_{eq} decreased abruptly with increasing C_W. This section of the

dx.doi.org/10.1021/la201009z |*Langmuir* 2011, 27, 8144–8152

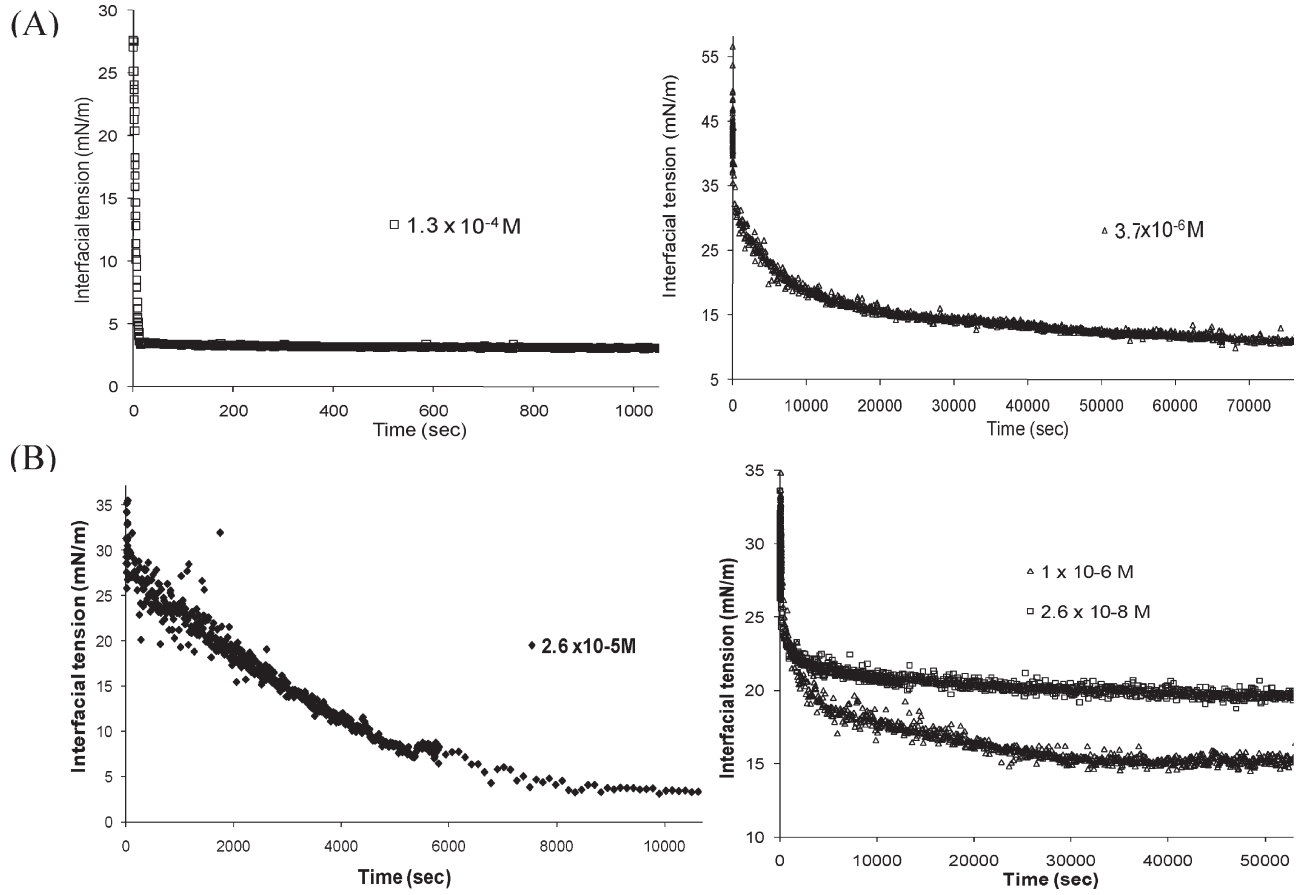

Figure 3. Interfacial tension kinetics measured at 40 °C and 90 bar of CO_2 for *F8H5*PC (A) and *F8H*11PC (B).

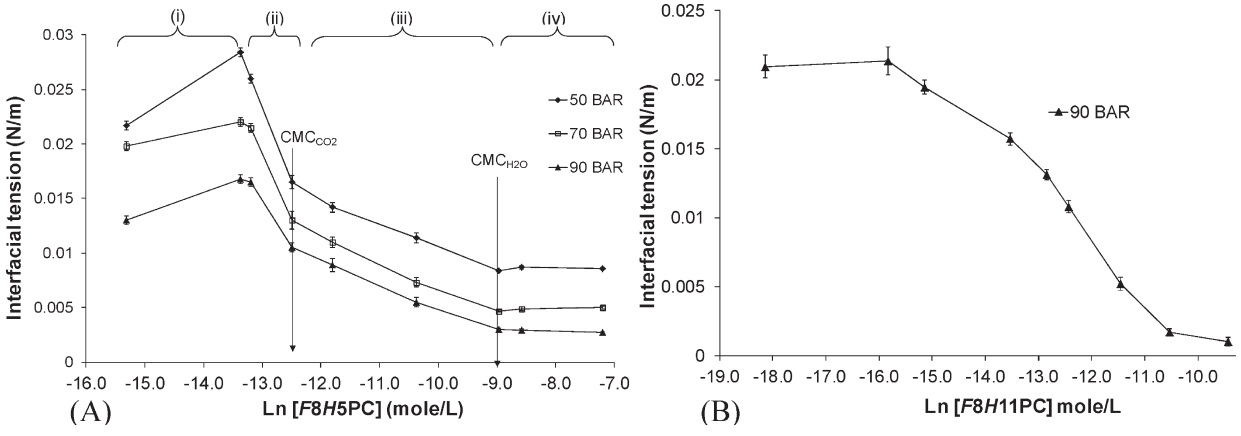

Figure 4. Gibbs isotherms: variation of γ_{eq} between H_2O and CO_2 as a function of C_W of *F8H5*PC (A) and *F8H*11PC (B) for various P_{CO2}.

isotherm is typical of a Gibbs monolayer. It shows the steepest slope of the four sections and allowed calculation of the maximal interfacial surfactant concentration as Gibbs monolayer (Γ_{max}) and then A_{min} (the minimal surface area occupied by the surfactant) using the Gibbs equation:

$$d\gamma = -nRT\Gamma \, d \ln C_W \qquad (6)$$

where $n = 1$ for zwitterionic molecules in the absence of other ions in the solution,[41] R is the perfect gas constant, and T is the temperature.

A_{min} increases from 31.5 to 35.5 Å^2 and then to 49.9 Å^2 as P_{CO2} increases from 50 to 70 and to 90 bar, respectively (Table 1). This demonstrates that the increase in P_{CO2} results in a decrease in the number of adsorbed *F8H5*PC molecules needed to attain the minimum energy state. This could be due to the decrease in γ_{eq} between pure H_2O and CO_2 that occurs as P_{CO2} increases within this pressure range (leading to a high CO_2 density change). The higher A_{min} values, calculated for P_{CO2} of 70 and 90 bar, indicate that CO_2 molecules might be intercalated between the *F*-surfactant tails, whereas the value of 31.5 Å^2

dx.doi.org/10.1021/la201009z |*Langmuir* 2011, 27, 8144–8152

Table 1. Minimal Surface Area Occupied by the Surfactant (A_{min}) and Critical Micelle Concentrations in Water (CMC_{H2O}) and in CO_2 (CMC_{CO2}) versus P_{CO2} for *F8H5*PC and *F8H11*PC As Calculated from Gibbs Isotherms Measured at 40 °C

	P_{CO2} (bar)	A_{min} (Å^2)	CMC_{CO2} (M)	CMC_{H2O} (M)
*F8H5*PC	50	31.5	3.7×10^{-6}	1.3×10^{-4}
	70	35.5		
	90	49.9		
*F8H11*PC	90	75.7		2.6×10^{-5}

obtained at 50 bar indicates that the fluorinated chains are in a compact state. The high solubility of CO_2 in fluorocarbons is well documented.[35] Furthermore, an increase in P_{CO2} could lead to an increase in the interactions between surfactant tails and CO_2 molecules because of the increase in CO_2 density. As a result, the tail−tail interactions decrease as P_{CO2} increases, which could explain the high A_{min} values obtained when increasing P_{CO2}. Therefore, the increase in P_{CO2} leads to an increase in A_{min} through two possible effects: on one hand, a better solvation by CO_2 of the surfactant tails leading to a reduction of the tail−tail interactions and, on the other hand, a contribution of the CO_2 molecules to the decrease of γ_{eq}. For various *F*-surfactants and at higher pressures than the maximal one allowed by our measuring system (100 bar), other studies have found higher A_{min} values than those we found at 90 bar. Thus, at 15 °C and 500 bar, Eastoe et al.[5] found an A_{min} of 90 Å^2 for the fluorinated AOT analogue di-HCF4. By comparing this value to that corresponding to the molecular area of AOT at a water/oil interface (60 Å^2), the authors concluded that the film packing requirements are generally lower in CO_2 systems than in hydrocarbon systems. They also found at 25 °C and 500 bar an A_{min} of 140 Å^2 for the hybrid surfactant $(C_7H_{15})(C_7F_{15})CHSO_4^-Na^+$.[7] By means of the same technique as ours and by plotting Gibbs isotherms, da Rocha and Johnston[22] studied the adsorption of the *F*-surfactant ($PFPECOO^-,NH_4^+$; 2500 g mol^{-1}) from the bulk CO_2 and found a A_{min} value of 96 Å^2 at 45 °C for a CO_2 density of 0.842 g L^{-1} (∼230 bar).

(iii) For C_W comprised between 4×10^{-6} and 1.3×10^{-4} M, a third regime, characterized by an inflection of the Gibbs isotherm and a less pronounced decrease in γ_{eq}, was observed (Figure 4A). Because of nonideality, the interface can no longer be described by the Gibbs equation. Such phenomena have already been observed by da Rocha et al.[22] at the CO_2-H_2O interface in the presence of $PFPECOO^-NH_4^+$ dissolved in the CO_2 phase. The authors interpreted this inflection as reflecting a critical microemulsion concentration "CμC" related to the formation, past this point, of a microemulsion phase, which reduces the number of surfactant molecules available for the interface, leading to a less marked decrease in γ_{eq}. Sagisaka et al.[36] determined the "CμC" of a sodium bis(1*H*,1*H*,2*H*,2*H*-heptadecafluorodecyl)-2-sulfosuccinate adsorbed at the CO_2-H_2O interface (40 °C and 250 bar) to be 1.9×10^{-7} M. Because of its relatively small size and fluorinated moiety, *F8H5*PC is soluble in both phases. When the total amount of *F8H5*PC added to the system increases, the surfactant concentration in both phases increases until saturation in unimer of the phase in which it is less soluble, i.e., the CO_2 phase. This saturation could lead to the formation of micelles. Hence, similarly to what da Rocha et al.[22] observed in another system, the reaching of saturation of the CO_2 phase with *F8H5*PC could result in an inflection of the Gibbs isotherm due to the sequestration of some molecules in micelles in the CO_2 phase. The *F8H5*PC C_W which induces saturation of the CO_2 phase is noted CMC_{CO2} in Figure 4A.

(iv) A fourth regime is observed for C_W higher than 1.3×10^{-4} M, for which γ_{eq} does no longer vary when C_W increases. This critical micelle concentration corresponds to the appearance of the first micelles in the aqueous phase (CMC_{H2O}). This is in the range of magnitude of the values obtained by Jackson et al.[37] for $C_8F_{17}C_6H_{12}N^+(CH_3)_3Br^-$ at the air−water interface. Above this concentration, the shape of the γ kinetics changes abruptly; particularly, the γ_{eq} values are rapidly reached (∼100 s). This change implies faster surfactant adsorption, which could be due to a change in the mode of surfactant transport from bulk water to the interface.

Contrary to those of *F8H5*PC, the Gibbs isotherm obtained for *F8H11*PC has a classical shape, with γ_{eq} decreasing until it reaches a minimum, after which it does no longer vary with increasing *F8H11*PC C_W (Figure 4B). The C_W above which γ_{eq} remains constant corresponds to the aqueous critical concentration for which micelles start to form in the aqueous phase (CMC_{H2O}). The CMC_{H2O} values obtained for *F8H11*PC (2.6×10^{-5} M) and *F*8H5PC (1.3×10^{-4} M) at 90 bar are in accordance with the relative solubilities of the two *F*-surfactants in water. The surfactant with the lowest water solubility (*F8H11*PC) forms micelles at the lowest C_W. The difference in shape of the isotherms of the two *F*-surfactants could be due to the impossibility for *F8H11*PC molecules to be extracted in the CO_2 phase due to their very low solubility. Additionally, the formation of a very cohesive interfacial layer above a given C_W could inhibit further extraction of *F8H11*PC into the CO_2 phase. Actually, above a C_W of 1.3×10^{-6} M, the *F8H11*PC molecules are very closely packed and interact strongly at the interface, as suggested by film collapse during compression of the interfacial area (Figure 7). Comparison of the A_{min} values obtained for *F8H11*PC (75.7 Å^2) and for *F8H5*PC (49.9 Å^2) at 90 bar shows that the surfactant having the longest hydrocarbon spacer occupies a larger area at the CO_2-H_2O interface (Table 1). This could be explained by the insertion of more CO_2 molecules between *F8H11*PC surfactant tails than for *F8H5*PC. Additionally, assuming that both surfactant tails are completely expanded in the CO_2 phase due to the favorable interaction of the fluorinated moieties with CO_2 molecules, the A_{min} values could suggest that the surfactant tails are tilted at the interface. Knowing the tail lengths and the area they occupy at the interface, tilt angles of 56° and 62.5° were calculated for *F8H5*PC and *F8H11*PC, respectively. These values are close to those found by Jackson et al.[37] for $C_8F_{17}C_6H_{12}N^+(CH_3)_3Br^-$ (65°) at the air/water interface. This difference in tilt angle shows that it is easier for *F8H11*PC molecules than for *F8H5*PC molecules to develop tail/tail interactions, even if the interfacial A_{min} occupied by *F8H11*PC is higher than for *F8H5*PC.

3.2. Interfacial Film Rheology. In a first approximation, we calculated the apparent elasticity ($E_a = (\Delta\gamma/\Delta A)A_i$) for C_W of the two surfactants (Figure 5A,B). In both cases, E_a increases with C_W up to a maximum and then decreases. The apparent elasticity is composed of an equilibrium part (E_e), linked to the conservation of the energy at the interface by the formation of interactions between surfactant molecules, and a nonequilibrium part (E_{ne}), linked to the dissipation rate of the energy from the interface, either by intrinsic reorganization of the interface or by

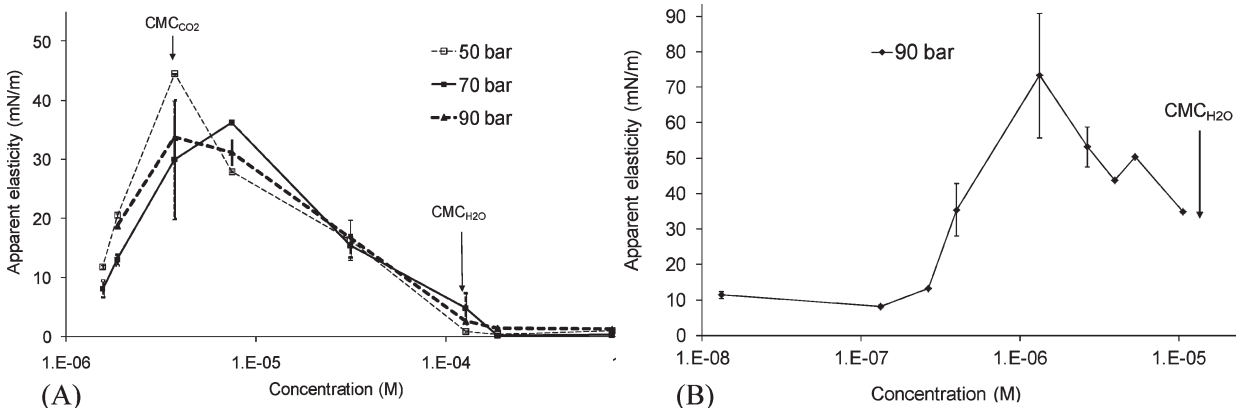

Figure 5. Variation of E_a vs C_W (log scale): (A) *F8H5*PC and (B) *F8H11*PC.

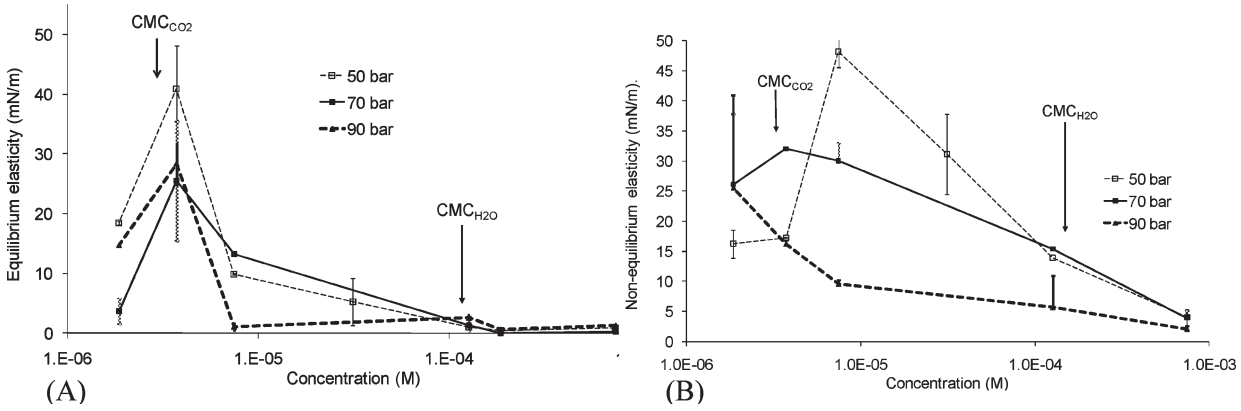

Figure 6. Variation of E_e (A) and E_{ne} (B) as a function of *F8H5*PC C_W (log scale).

expulsion of surfactant molecules. These two parts are characteristics of the interface and do not depend on experimental conditions (e.g., compression rate). For clarity, we will discuss separately the rheological behavior of each surfactant.

(i) In the case of *F8H5*PC, E_a varies similarly as a function of C_W for the three P_{CO2} investigated. Maximum E_a values are obtained for C_W close to CMC_{CO2}. After this maximum, E_a decreases monotonously until reaching a minimum close to zero, around C_W equal to CMC_{H2O}. Above this C_W, E_a does not vary anymore.

The variation of E_e as a function of *F8H5*PC C_W is presented in Figure 6A. As for E_a, E_e varies in a similar manner with C_W for the three P_{CO2} investigated and presents a maximum for a C_W equal to the CMC_{CO2}. Contrary to E_a and E_e, the evolution of E_{ne} with *F8H5*PC C_W changes with P_{CO2} (Figure 7B). At 50 bar, E_{ne} remains constant until C_W is equal to the CMC_{CO2}. Then, E_{ne} sharply increases up to a maximum of 48 mN/m followed by a monotonous decrease to values close to 5 mN/m for C_W lower than the CMC_{H2O}. At 70 bar, the E_{ne} values obtained below CMC_{CO2} are higher than those obtained at 50 bar but decrease monotonously at higher concentrations. At 90 bar, E_{ne} decreases continuously with a slope that diminishes as C_W increases.

E_e is linked to lateral interactions between the *F8H5*PC molecules adsorbed at the interface. Below a given state of compaction, the closer the surfactant molecules, the larger the increase in lateral interactions upon compression. Therefore, the increase in E_e values measured for a *F8H5*PC C_W lower than CMC_{CO2} can be related to augmented interactions between the *F8H5*PC tails (Figure 6A). The values of E_{ne} measured for C_W lower than CMC_{CO2} (15 and 25 mN/m for a P_{CO2} of 50 and 70−90 bar, respectively) illustrate the presence of interactions between surfactant molecules and the adjacent phases, possibly leading to expulsion of surfactant molecules upon compression. The fact that, in this range of C_W the E_e values at 50 bar were higher than at 90 bar, while the E_{ne} values at 50 bar are lower than at 90 bar, shows that the surfactant/surfactant interactions are higher at 50 bar than at 90 bar and that the surfactant/solvents (CO_2 or H_2O) interactions are higher at 90 bar than at 50 bar.

The maximal E_e is given by the initial surfactant compaction state allowing maximal increase in surfactant interaction for a given relative reduction of the area. Figure 6A shows that for the three P_{CO2} studied this initial compaction state corresponds to the maximal state compaction of *F8H5*PC as a Gibbs monolayer. Furthermore, the fact that the maximal E_e value obtained at 50 bar is higher than that obtained at 70 and 90 bar shows that the initial interfacial state leading to the higher tail−tail interaction corresponds to a state in which the surfactant molecular area is equal to the minimal molecular area calculated for 50 bar (31.5 Å^2), since the molecular area calculated for 70 and 90 bar are higher (respectively 35.5 and 49.9 Å^2).

Therefore, the sharp decrease in E_e that occurs just after the maximum (at CMC_{CO2}) is not due to an overreaching of the initial interfacial state leading to the maximal tail−tail interactions induced by area compression. This steep diminution of E_e can be associated with a rapid reorganization of the interface. This reorganization can consist in the expulsion of a large

dx.doi.org/10.1021/la201009z |*Langmuir* 2011, 27, 8144–8152

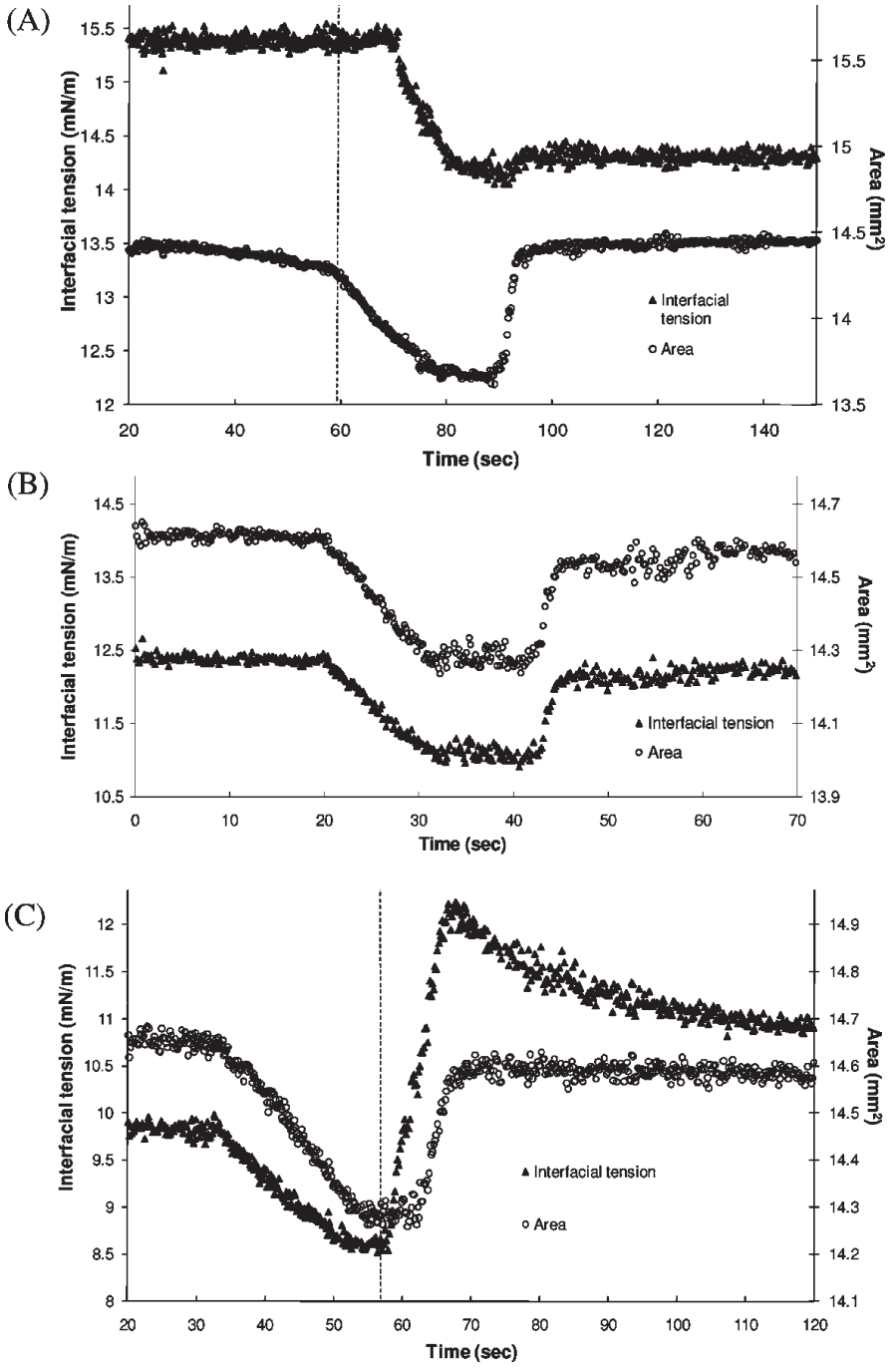

Figure 7. Variation of γ during a slow compression of the interfacial area, followed by a return to the initial area obtained for *F8H11*PC C_W equal to 1.3×10^{-6} M (A), 2.6×10^{-6} M (B), and 5.2×10^{-6} M (C).

number of *F8H5*PC molecules into the phase in which the chemical potential of the surfactant is the lowest, due to the high initial compaction of the interface and due to the fact that no increase in interactions among tails occurs during compression as E_e is close to zero. Furthermore, the increase in P_{CO2} facilitates this reorganization, since it induces a decrease in E_{ne}. Also, the decrease in E_{ne} when C_W increases indicates easier expulsion of surfactant molecules.

Above CMC_{H2O}, the low value of E_{ne}, concomitant with the low value of E_e, suggests very fast and easy expulsion of *F*-surfactants that could occur toward the two phases simultaneously due to high flexibility of the interfacial layer. This flexibility of the interface could be due to its reorganization in structures similar to the hemimicelles found with semifluorinated alkanes adsorbed at the air/water interface.[38−40] This flexibility could facilitate the expulsion of surfactant molecules from the interface to the bulk water and, during the γ kinetics, facilitate the adsorption of *F*-surfactants from the bulk water phase, explaining the very short time necessary to reach γ_{eq}. For instance, *F*-surfactants could be adsorbed as micelles formed above the CMC_{H2O}. This phenomenon involves reorganization between micelles and the interfacial monolayer, allowing their "fusion".[41]

dx.doi.org/10.1021/la201009z |*Langmuir* 2011, 27, 8144–8152

However, these micelles would probably be different from those observed with semifluorinated alkanes adsorbed at the air/water interface[38−40] because the latter micelles were found to be very large and stable and have slow dynamics. Their formation would likely not facilitate passage of the surfactant from one phase to the other. Also, above the CMC_{CO2}, the expulsion of *F*-surfactants from the interface could occur toward the CO_2 phase as micelles or microemulsion droplets. The energy needed for the *F*-surfactants to pass from an interfacial organization to a micelle state can be provided by the interfacial compression and could result from the formation of the hemimicelles.

The origin of the film flexibility and facilitated exchanges in those conditions of concentration and pressure may involve organized interfacial structures that should be analyzed by other techniques. Unfortunately, these analyses remain difficult to perform at a pressurized CO_2-H_2O interface. Such a flexible interface should be suitable to the formation of microemulsion.

(ii) Contrarily to *F8H5*PC, the interfacial films made of *F8H11*PC were purely elastic until C_W reached 2.6×10^{-6} M. As for *F8H5*PC, the E_a values observed for *F8H11*PC (Figure 5B) were low (∼10 mN/m) for the low C_W and then increased until a maximum is observed for C_W of 1.3×10^{-6} M. However, the maximum E_a obtained with *F8H11*PC is twice higher than with *F8H5*PC at the same P_{CO2}. After the maximum, E_a slightly decreases until *C* is close to CMC_{H2O}. Measurement of E_a for higher C_W values was not possible due to the low value of γ_{eq} (1 mN/m), which did not allow compression of the water drop. Compared to *F8H5*PC, E_a remained high even when the *F8H11*PC C_W was close to the CMC_{H2O}.

Interestingly, we observed typical behaviors depending on C_W as illustrated by the difference in γ variation that occurs upon slow variation of the interfacial area (Figure 7). For a C_W of 1.3×10^{-6} M (Figure 7A), the reduction of the interfacial area leads to a strong reduction of γ, as indicated by the high E_a value. Furthermore, a time lag (∼8 s) between the interfacial area reduction and the response of the interface, i.e., a reduction of γ, is observed. This time lag could be attributed to the low *F8H11*PC Γ value obtained at this C_W. For this C_W, some space exists between the adsorbed *F8H11*PC molecules, as shown by the coverage degree (Γ/Γ_{max}) of 65% calculated from the Gibbs isotherm (Figure 4B). The interfacial area reduction results in bringing the surfactant molecules nearer together, followed by an increase in their interaction and, consequently, to a strong decrease in γ value. The return to the initial area induced no change in γ, indicating that the interface is in a steady state. The constant γ value obtained during the dilatation of the interfacial area can be explained by the concomitant adsorption of *F8H11*PC molecules due to a lower characteristic time needed for surfactant adsorption as compared to the characteristic time for the adsorbed compacted surfactant to respread on the interface. The fact that the adsorption rate is higher than the respreading rate shows that area reduction leads to strong interactions between surfactant tails, as in a collapsed state. This can be attributed to the length of the surfactant tails and could modify *F8H11*PC extraction in the CO_2 phase.

At a *F8H11*PC C_W of 2.6×10^{-6} M (Figure 7B), the reduction of γ during the slow droplet compression experiment is less pronounced than at 1.3×10^{-6} M, as shown by a lower E_a value (Figure 5B). In this case, the variation of the interfacial area and of γ is completely synchronized. Furthermore, the fast drop area compression (data not shown) induced no relaxation phenomenon of the interface, showing the absence of expulsion of surfactant and a purely elastic behavior of the interface. For this C_W, the interface starts to be saturated with surfactant molecules, as shown by the coverage degree of 76%, implying that the surfactant molecules are closer to each other than at 1.3×10^{-6} M. The compression of the drop area induces a slight gathering between the adsorbed surfactant molecules and a slight increase in their degree of interaction, which was already important. Therefore, the reduction of γ was lower than at 1.3×10^{-6} M. When expanding the drop area to the initial area, γ returns to its initial value due to the constant composition of the interface compared to its state before compression, which implies that there was no or little free space for the adsorption of additional surfactant.

At a *F8H11*PC C_W of 5.2×10^{-6} M (Figure 7C) the interfacial area is more saturated in surfactant molecules (coverage degree of 86%), and the reduction of the interfacial area induces a similar decrease in γ as for a C_W of 2.6×10^{-6} M, leading to similar E_a values. As the interface is almost completely saturated with *F8H11*PC, the compression results in the expulsion of surfactant molecules in the phase where they are most soluble (aqueous phase). This expulsion induces an increase in γ before the redilatation of the interfacial area and the readsorption of surfactant molecules after the dilatation of the interface back to the initial area. This observation is comforted by the interfacial relaxation phenomenon that occurs during the rapid interfacial area reduction (data not shown), indicating the appearance of viscoelastic properties characterized by an E_{ne} value of 75.4 ± 21 mN/m and a τ of 17.1 ± 6.9 s.

4. CONCLUSIONS

We have analyzed the behavior of two partially fluorinated surfactants, *F8H5*PC and *F8H11*PC, at the CO_2-H_2O interface in order to assess the influence of the hydrocarbon spacer that links their CO_2-philic perfluoroalkyl tail to their hydrophilic phosphocholine headgroup. The change of the number of carbon atoms in the spacer from 5 to 11 induces a strong modification of their behavior at this interface as well as in the bulk CO_2 and H_2O phases. The nonclassical shape of the Gibbs isotherm and high flexibility of the interface suggests that the shorter *F8H5*PC surfactant could form micelles in both water and CO_2 phases. At high bulk water concentrations, this *F*-surfactant forms an interfacial layer that does not respect the Gibbs ideality. This particular interfacial behavior also allows rapid interfacial adsorption of *F8H5*PC.

The longer *F*-surfactant (*F8H11*PC) forms micelles only in the water phase and leads to a classical Gibbs interface. This surfactant is able to decrease γ_{eq} down to 1 mN/m and forms a strongly elastic interface. As this surfactant forms a highly cohesive interface, it should be able to prevent the coalescence W/C emulsion droplets. The finding of a dramatic effect of the length of the hydrocarbon spacer in partially fluorinated surfactants on interfacial tension and film elasticity could help control the formation of microemulsions versus emulsions of water in CO_2 and should help elaborate a rationale for the design of surfactants specifically adapted to this medium.

AUTHOR INFORMATION

Corresponding Author

*E-mail: frank.boury@univ-angers.fr. Phone: +332 44 68 85 28. Fax: +332 44 68 85 46.

REFERENCES

(1) Jacobson, G. B.; Lee, C. T.; Johnston, K. P.; Tumas, W. Enhanced Catalyst Reactivity and Separations Using Water/Carbon Dioxide Emulsions. *J. Am. Chem. Soc.* **1999**, *121* (50), 11902–11903.

(2) Lee, C. T., Jr.; Psathas, P. A.; Johnston, K. P.; DeGrazia, J.; Randolph, T. W. Water-in-carbon dioxide emulsions: Formation and stability. *Langmuir* **1999**, *15* (20), 6781–6791.

(3) da Rocha, S. R. P.; Harrison, K. L.; Johnston, K. P. Effect of Surfactants on the Interfacial Tension and Emulsion Formation between Water and Carbon Dioxide. *Langmuir* **1999**, *15* (2), 419–428.

(4) Psathas, P. A.; Janowiak, M. L.; Garcia-Rubio, L. H.; Johnston, K. P. Formation of carbon dioxide in water miniemulsions using the phase inversion temperature method. *Langmuir* **2002**, *18* (8), 3039–3046.

(5) Eastoe, J.; Cazelles, B. M. H.; Steytler, D. C.; Holmes, J. D.; Pitt, A. R.; Wear, T. J.; Heenan, R. K. Water-in-CO_2 microemulsions studied by small-angle neutron scattering. *Langmuir* **1997**, *13* (26), 6980–6984.

(6) Boury, F.; Benoit, J.-P.; Thomas, O.; Tewes, F. Method for preparing particles from an emulsion in supercritical or liquid CO_2. WO07072106, 28-06-2007, 2007.

(7) Eastoe, J.; Bayazit, Z.; Martel, S.; Steytler, D. C.; Heenan, R. K. Droplet structure in a water-in-CO_2 microemulsion. *Langmuir* **1996**, *12* (6), 1423–1424.

(8) Stone, M. T.; Smith, P. G., Jr.; Da Rocha, S. R. P.; Rossky, P. J.; Johnston, K. P. Low Interfacial Free Volume of Stubby Surfactants Stabilizes Water-in-Carbon Dioxide Microemulsions. *J. Phys. Chem. B* **2004**, *108* (6), 1962–1966.

(9) Chaitanya, V. S. V.; Senapati, S. Self-Assembled Reverse Micelles in Supercritical CO2 Entrap Protein in Native State. *J. Am. Chem. Soc.* **2008**, *130* (6), 1866–1870.

(10) Holmes, J. D.; Steytler, D. C.; Rees, G. D.; Robinson, B. H. Bioconversions in a Water-in-CO_2 Microemulsion. *Langmuir* **1998**, *14* (22), 6371–6376.

(11) Johnston, K. P.; Harrison, K. L.; Clarke, M. J.; Howdle, S. M.; Heitz, M. P.; Bright, F. V.; Carlier, C.; Randolph, T. W. Water-in-carbon dioxide microemulsions: An environment for hydrophiles including proteins. *Science* **1996**, *271* (5249), 624–626.

(12) Eastoe, J.; Dupont, A.; Steytler, D. C. Fluorinated surfactants in supercritical CO_2. *Curr. Opin. Colloid Interface Sci.* **2003**, *8* (3), 267–273.

(13) Hoefling, T.; Stofesky, D.; Reid, M.; Beckman, E.; Enick, R. M. The incorporation of a fluorinated ether functionality into a polymer or surfactant to enhance CO_2-solubility. *J. Supercrit. Fluids* **1992**, *5* (4), 237–241.

(14) Hoefling, T. A.; Enick, R. M.; Beckman, E. J. Microemulsions in near-critical and supercritical carbon dioxide. *J. Phys. Chem.* **1991**, *95* (19), 7127–7129.

(15) Psathas, P. A.; da Rocha, S. R. P.; Lee, C. T.; Johnston, K. P.; Lim, K. T.; Webber, S. Water-in-Carbon Dioxide Emulsions with Poly(dimethylsiloxane)-Based Block Copolymer Ionomers. *Ind. Eng. Chem. Res.* **2000**, *39* (8), 2655–2664.

(16) Sarbu, T.; Styranec, T. J.; Beckman, E. J. Design and synthesis of low cost, sustainable CO2-philes. *Ind. Eng. Chem. Res.* **2000**, *39* (12), 4678–4683.

(17) Temtem, M.; Casimiro, T.; Santos, A. G.; Macedo, A. L.; Cabrita, E. J.; Aguiar-Ricardo, A. Molecular Interactions and CO2-Philicity in Supercritical CO2. A High-Pressure NMR and Molecular Modeling Study of a Perfluorinated Polymer in scCO2. *J. Phys. Chem. B* **2007**, *111* (6), 1318–1326.

(18) Harrison, K.; Goveas, J.; Johnston, K. P.; O'Rear Iii, E. A. Water-in-carbon dioxide microemulsions with a fluorocarbon-hydrocarbon hybrid surfactant. *Langmuir* **1994**, *10* (10), 3536–3541.

(19) Keiper, J. S.; Simhan, R.; DeSimone, J. M.; Wignall, G. D.; Melnichenko, Y. B.; Frielinghaus, H. New phosphate fluorosurfactants for carbon dioxide. *J. Am. Chem. Soc.* **2002**, *124* (9), 1834–1835.

(20) Eastoe, J.; Paul, A.; Downer, A.; Steytler, D. C.; Rumsey, E. Effects of fluorocarbon surfactant chain structure on stability of water-in-carbon dioxide microemulsions. Links between aqueous surface tension and microemulsion stability. *Langmuir* **2002**, *18* (8), 3014–3017.

(21) Heitz, M. P.; Carlier, C.; DeGrazia, J.; Harrison, K. L.; Johnston, K. P.; Randolph, T. W.; Bright, F. V. Water core within perfluoropolyether-based microemulsions formed in supercritical carbon dioxide. *J. Phys. Chem. B* **1997**, *101* (34), 6707–6714.

(22) da Rocha, S. R. P.; Johnston, K. P. Interfacial thermodynamics of surfactants at the CO_2-water interface. *Langmuir* **2000**, *16* (8), 3690–3695.

(23) Krafft, M. P.; Riess, J. G. Chemistry, physical chemistry, and uses of molecular fluorocarbon- hydrocarbon diblocks, triblocks, and related compounds-unique "apolar" components for self-assembled colloid and interface engineering. *Chem. Rev.* **2009**, *109* (5), 1714–1792.

(24) Krafft, M. P.; Riess, J. G. Highly fluorinated amphiphiles and colloidal systems, and their applications in the biomedical field. A contribution. *Biochimie* **1998**, *80* (5−6), 489–514.

(25) Krafft, M. P. Fluorocarbons and fluorinated amphiphiles in drug delivery and biomedical research. *Adv. Drug Delivery Rev.* **2001**, *47* (2−3), 209–228.

(26) Courrier, H. M.; Vandamme, T. F.; Krafft, M. P. Reverse water-in-fluorocarbon emulsions and microemulsions obtained with a fluorinated surfactant. *Colloids Surf., A* **2004**, *244* (1−3), 141–148.

(27) Sadtler, V. M.; Giulieri, F.; Krafft, M. P.; Riess, J. G. Micellization and adsorption of fluorinated amphiphiles: Questioning the 1 CF_2 j 1.5 CH_2 rule. *Chem.—Eur. J.* **1998**, *4* (10), 1952–1956.

(28) Krafft, M. P.; Rolland, J. P.; Vierling, P.; Riess, J. G. New perfluoroalkylated phosphocholines, Effects on particle size and stability of fluorocarbon emulsions. *New J. Chem.* **1990**, *14*, 869–875.

(29) Tewes, F.; Boury, F. Thermodynamic and dynamic interfacial properties of binary carbon dioxide-water systems. *J. Phys. Chem. B* **2004**, *108* (7), 2405–2412.

(30) Tewes, F.; Boury, F. Effect of H_2O-CO_2 organization on ovalbumin adsorption at the supercritical CO_2-water interface. *J. Phys. Chem. B* **2005**, *109* (5), 1874–81.

(31) Tewes, F.; Boury, F. Dynamic and rheological properties of classic and macromolecular surfactant at the supercritical CO_2-H_2O interface. *J. Supercrit. Fluids* **2006**, *37* (3), 375–383.

(32) Boury, F.; Ivanova, T.; Panaïotov, I.; Proust, J. E.; Bois, A.; Richou, J. Dilatational properties of adsorbed poly(D,L-lactide) and bovine serum albumin monolayers at the dichloromethane/water interface. *Langmuir* **1995**, *11* (5), 1636–1644.

(33) Boury, F.; Ivanova, T.; Panaïotov, I.; Proust, J. E.; Bois, A.; Richou, J. Dynamic Properties of Poly(DL-lactide) and Polyvinyl Alcohol Monolayers at the Air/Water and Dichloromethane/Water Interfaces. *J. Colloid Interface Sci.* **1995**, *169* (2), 380–392.

(34) Lehmkühler, F.; Paulus, M.; Sternemann, C.; Lietz, D.; Venturing, F.; Gutt, C.; Tolan, M. The carbon dioxide-water interface at conditions of gas hydrate formation. *J. Am. Chem. Soc.* **2009**, *131* (2), 585–589.

(35) Riess, J. G. Oxygen carriers ("blood substitutes") - Raison d'etre, chemistry, and some physiology. *Chem. Rev.* **2001**, *101* (9), 2797–2919.

(36) Sagisaka, M.; Fujii, T.; Koike, D.; Yoda, S.; Takebayashi, Y.; Furuya, T.; Yoshizawa, A.; Sakai, H.; Abe, M.; Otake, K. Surfactant-mixing effects on the interfacial tension and the microemulsion formation in water/supercritical CO_2 system. *Langmuir* **2007**, *23* (5), 2369–2375.

(37) Jackson, A. J.; Li, P. X.; Dong, C. C.; Thomas, R. K.; Penfold, J. Structure of partially fluorinated surfactant monolayers at the air - Water interface. *Langmuir* **2009**, *25* (7), 3957–3965.

(38) Maaloum, M.; Muller, P.; Krafft, M. P. Monodisperse surface micelles of nonpolar amphiphiles in langmuir monolayers. *Angew. Chem., Int. Ed.* **2002**, *41* (22), 4331–4334.

(39) Maaloum, M.; Muller, P.; Krafft, M. P. Lateral and Vertical Nanophase Separation in Langmuir-Blodgett Films of Phospholipids and Semifluorinated Alkanes. *Langmuir* **2004**, *20* (6), 2261–2264.

(40) Zhang, G.; Marie, P.; Maaloum, M.; Muller, P.; Benoit, N.; Krafft, M. P. Occurrence, shape, and dimensions of large surface hemimicelles made of semifluorinated alkanes. Elongated versus circular hemimicelles. Pit- and tip-centered hemimicelles. *J. Am. Chem. Soc.* **2005**, *127* (29), 10412–10419.

(41) Chiu, Y. C.; Kuo, P. R. An empirical correlation between low interfacial tension and micellar size and solubilization for petroleum sulfonates in enhanced oil recovery. *Colloids Surf., A* **1999**, *152* (3), 235–244.